

Pier: Efficient Large Language Model pretraining with Relaxed Global Communication

Shuyuan Fan

Department of Electrical and Computer Engineering
Rutgers University
New Brunswick, United States
sf850@scarletmail.rutgers.edu

Zhao zhang

Department of Electrical and Computer Engineering
Rutgers University
New Brunswick, United States
zhao.zhang@rutgers.edu

Abstract—Global communication, such as all-reduce and all-gather, is the prominent performance bottleneck in large language model (LLM) pretraining. To address this issue, we present Pier, an efficient and scalable optimizer with relaxed global communication. Pier is built upon DiLoCo, which leverages an inner optimizer within groups of processors and an outer optimizer that requires global communication. To preserve the convergence and model performance, Pier incorporates two key techniques for the outer optimizer: momentum warmup and momentum decay. Pier employs an efficient and scalable system architecture to enable complex parallelization strategies in LLM pretraining. We examine the model performance and runtime reduction of Pier using the GPT model family (e.g., small, medium, XL, and 7B) and the OpenWebText dataset with a suite of thirteen downstream tasks. With data parallel strategy, Pier speeds up GPT-2 XL training by up to 2.7x-3.7x on 256 NVIDIA A100 GPUs and 1.2x-1.9x on 64 GH200 Superchips, respectively, without degradation of validation loss or downstream task performance. With data parallel and tensor parallel, Pier reduces the time cost GPT-2 7B model training by 54.5% on 128 A100s.

Index Terms—machine learning, distributed computing, high performance computing

I. INTRODUCTION

Major stakeholders are designing large language models (LLMs) with ever-increasing size, driven by the scaling law [1], which states that the model’s capability improves with scale. The state-of-the-art LLMs [2]–[4] are trained with tens of thousands of high-end graphic processing units (GPUs) in complex distributed strategies, including data parallel [5], tensor parallel [6], pipeline parallel [7], [8], and context parallel [9]. Communication is the prominent bottleneck in LLM pretraining, as simply evidenced by the low scaling efficiency of 42.7% and 34.6% for GPT-2 1.5B training with 32 NVIDIA A100s and 64 NVIDIA GH200 superchips using the AdamW optimizer with standard data parallel, respectively (see AdamW curves in Figure 7).

To reduce communication costs and boost scaling efficiency for LLM pretraining, researchers have proposed algorithms that fall into two categories. The first category lowers the communication volume via gradient sparsity [10], [11] and quantization [12]. And the second category reduces the global communication frequency by exploiting optimizers such as local SGD [13]. With the hard constraints of model performance (i.e., validation loss and downstream task performance),

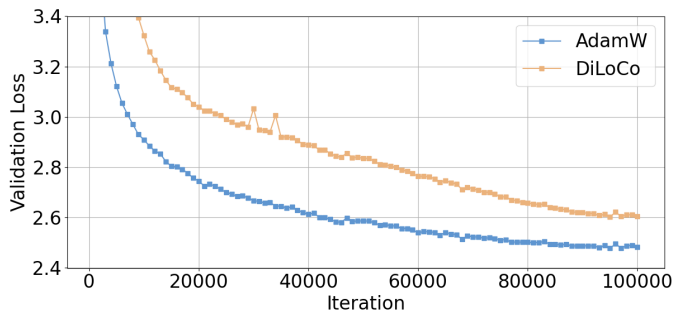


Fig. 1. Validation Loss Comparison between AdamW (8 GPUs, Fully Synchronized) and DiLoCo (8 Groups, 1 GPU per Group) During the Pretraining of GPT-2 XL Model.

methods in the first category exhibit modest improvements of 10-30% [11], [14]. Although the methods with relaxed global communication show great potential in pretraining acceleration, they suffer from performance degradation. Among these methods, DiLoCo [15] introduces a two-layer optimization framework that partitions GPUs into groups. It utilizes an inner optimizer that only requires intra-group communication and an outer optimizer that requires inter-group (i.e., global) communication. However, our empirical evaluation in Figure 1 shows degraded validation loss and downstream task performance using the GPT-2 XL model and OpenWebText dataset [16].

Our analysis of DiLoCo reveals that the gradient oscillation at the switching point from AdamW to DiLoCo is the root cause of performance degradation. This insight motivates the design of Pier, which incorporates two key techniques: momentum warmup and momentum decay for the outer optimizer. The momentum warmup technique tracks the model changes as the outer optimizer’s gradients, for every few iterations during the so-called “lazy start” phase in DiLoCo, where the model is updated by using the same AdamW as baseline. After the “lazy start” phase, the momentum decay technique exploits a fixed schedule to gracefully migrate from AdamW to DiLoCo. To reduce the memory overhead in the outer optimizer, Pier offloads the model and optimizer states to host memory during inner loops. Pier enables the overlay of data parallel over tensor parallel to support larger models, where the outer step parallelizes communication and model updates.

Pier is implemented upon the Megatron-LM framework. We evaluate the design effectiveness of Pier using the GPT-2 model family, including small (125M), medium (345M), XL (1.5B), and a 7B model with the OpenWebText dataset. We examine the convergence and downstream task performance of Pier using a suite of thirteen tasks. With the model performance guarantee, we conduct five studies on the scaling patterns of Pier. We first perform a weak scaling study to identify the global batch size boundary of Pier with a fixed token budget and group sizes. The second study explores the convergence boundary when increasing the synchronization interval of the outer optimizer. We then perform a strong scaling study to determine the scaling efficiency boundary of Pier with fixed global batch sizes and the number of groups. In the fourth experiment, we vary the group size (i.e., the number of GPUs in a group) and fix the global batch size to study the impact of the number of groups on training speed. In the fifth study, we perform a mixed parallelism scaling experiment to examine the scalability of Pier for larger models.

We run the experiments on two GPU clusters: NERSC Perlmutter and TACC Vista. Pier shows comparable validation loss and downstream task performance with the baseline AdamW optimizer in standard data parallelism for GPT-2 small, medium, and XL. On Perlmutter, Pier speeds up GPT-2 small, medium, and XL training by 1.7x, 2.6x, and 2.7x with the maximum data parallel scale that guarantees model performance. If global communication is further relaxed, the speedup for GPT-2 XL can be as high as 3.7x on 256 A100s. On Vista, Pier is effective on GPT-2 XL with data parallel. The speedup is 1.2-1.9x on 128 GH200s. For GPT-2 7B training with data parallel and tensor parallel, Pier exhibits a speedup of 2.2x on 128 A100s.

The contributions of this paper are:

- The momentum warmup and momentum decay techniques that allow Pier to achieve comparable model performance as AdamW.
- The efficient Pier design that combines data parallel and tensor parallel.
- The comprehensive model performance evaluation with thirteen downstream tasks.
- The quantified end-to-end LLM pretraining time improvement over two production supercomputers with different GPUs and interconnect architectures.

II. BACKGROUND

In this section, we introduce the basic concepts of distributed LLM pretraining strategies, the communication bottleneck due to bandwidth hierarchy, and the structure of the DiLoCo optimizer.

A. Distributed Model Training

Modern LLM pretraining exploits complex parallelism strategies. 3D parallelism partitions a model across processors by layering data parallelism (DP) over pipeline and tensor parallelism (PP and TP). GPUs are partitioned into groups (Data Parallel Rank), and each group hosts a complete copy

of the model. Inside each group, the model is spread across nodes by layers to form the pipeline stages; Inside each node, layers (tensors) are evenly distributed across multiple GPUs, a technique referred to as tensor parallelism. With the data parallel approach, the only communications are the broadcast at the start of training and the gradient exchange in each iteration. In contrast, 3D parallelism requires intra- and inter-node communication for both forward and backward computation.

With the need for larger context in LLMs, long sequence support is introduced as a fourth dimension. Researchers have designed context parallelism (CP) with various partitioning and communication strategies over the query, key, and value matrices [9], [17], [18]. In addition, mixture-of-expert (MoE) models can leverage the expert parallelism (EP), where each expert is a standalone LLM. These distributed LLM pretraining strategies complicate the design of optimizers, as the models and optimizer states are spread across GPUs. In Pier, we design an efficient parallel strategy for the communication in the outer optimizer under TP and DP.

B. Bandwidth Hierarchy in Networks

State-of-the-art supercomputers are equipped with networks that feature hierarchical bandwidth. Within a compute node, GPUs are usually connected via NVLink, Infinity Fabric, or Xe Link. E.g., NVLink 4.0 and 5.0 support a bandwidth of 900 GB/s and 1.8 TB/s, respectively. These supercomputers deploy Infiniband or Slingshot to connect a massive number of compute nodes. E.g., the Infiniband NDR offers 100 GB/s bandwidth and HDR offers 50 GB/s. The global communication over the interconnects is the scaling bottleneck for LLM pretraining at extreme scale. This is because the all-reduce or all-gather is needed in every iteration. However, there exists an opportunity for lower communication cost if an optimizer can efficiently leverage the high bandwidth in the intra-node links. This hierarchical bandwidth in the supercomputer networks motivates the design of Pier.

C. DiLoCo

DiLoCo was motivated by the federated learning scenario, where the network bandwidth is extremely limited across different geolocations. It forms groups based on the geographical locations of the workers, exploits a two-layer optimization approach. In the inner loop, the model is trained with AdamW leveraging standard DP. The gradient synchronization is within each group, thus eliminating the global communication, which results in model parameter divergence across groups. Thus, for every few iterations (i.e., inner loop interval), the outer optimizer needs to gather the model weights from all groups and treat the model changes as gradients. Then the outer optimizer takes an optimization step to update the model and synchronize the model across groups. Empirically, Nesterov SGD shows better performance than SGD, momentum SGD, and AdamW as an outer optimizer [15].

III. RELATED WORKS

Researchers have studied various methods to reduce the communication overhead in LLM pretraining. These methods can be classified into two categories: lowering communication volume and reducing the frequency of communication.

A. Volume Reduction

The data compression approach is one of the most effective approaches for reducing communication cost in distributed deep learning. The early work [19] introduces 1-bit SGD with an error feedback mechanism to compensate for errors. It maintains convergence while reducing communication cost. Another technique used in gradient compression is sparsity, which communicates gradients with large magnitudes rather than transmitting all the gradients. EF21 [20] improves the classical error feedback mechanism, achieving both theoretical and practical convergence. Variance-based Gradient Compression [21] only transmits gradient entries that are unambiguous, while keeping ambiguous components local, effectively balancing compression and accuracy. Deep Gradient Compression (DGC) [10] combines several practical mechanisms, including warm-up, local gradient clipping, momentum correction, and sparsification into a unified framework. Moving beyond quantization and sparsification, PowerSGD [22] compresses gradients through low-rank matrix approximation, providing a communication-efficient approach suitable for large-scale machine learning systems. In practice, with the constraint of model performance (i.e., validation loss and downstream task performance), compression techniques [11], [14] can reduce the time cost by 10-20%.

B. Reducing Communication Frequency

Another series of works aims at reducing the frequency of communication. Local SGD [13] updates models on local workers every a few iterations, and synchronizes the diverged models across different workers via averaging model weights. This idea is widely adopted in federated learning. The later work [23] implements a unified theoretical framework for Local SGD and other federated learning approaches, and provides a convergence analysis under both *i.i.d.* and *non-i.i.d.* data settings.

DiLoCo [15] shows great potential in global communication reduction for pretraining of the decoder-only LLMs by partitioning GPUs into groups and synchronizing periodically. A follow-up research [24] presents a scalability analysis of DiLoCo, claiming better model performance with DiLoCo than AdamW for larger models. However, this study only shows the evidence of lower validation loss, which overlooks the downstream tasks. SparseLoCo [25] enhances communication efficiency further by applying top-k sparsification and quantization during the global synchronization step, achieving sparsity as low as $\tilde{1}$ -3%. It outperforms the AdamW and DiLoCo baseline in communication volume, validation loss, and three downstream tasks. Streaming-DiLoCo [26] improves DiLoCo by (1) synchronizing only subsets of the model parameters to reduce the peak communication demand; (2)

Algorithm 1 MomentumWarmup

Input: Training Iteration T

Input: Warmup percentage p

Input: Synchronization interval r

Initialize: Momentum coefficient μ

Initialize: Model parameters θ

Initialize: Momentum buffer M

Output: Updated model parameters θ_{pT}

Output: Momentum buffer M

```
1: for  $t = 1$  to  $pT$  do
2:   Compute local gradient  $\nabla_{\theta}$ 
3:    $\theta_t \leftarrow \text{OptimizerUpdate}(\theta_{t-1}, \nabla_{\theta})$ 
4:   if  $t \bmod r = 0$  then
5:      $\Delta\theta \leftarrow \theta_t - \theta_{t-r}$ 
6:      $M \leftarrow \mu M + \Delta\theta$ 
7:   end if
8: end for
```

overlapping communication and computation; (3) applying low-precision quantization for outer optimizer updates. While these approaches can reduce communication cost, the convergence and model performance is only evaluated with a few metrics. These studies also lack quantified measurements of communication time reduction in end-to-end pretraining on production supercomputers.

In contrast, Pier places convergence and model performance as the top priority. Pier integrates two techniques to preserve training convergence and downstream task performance, which is the hard constraint for the study of scalability and training time reduction.

IV. ALGORITHM AND SYSTEM DESIGN

In this section, we introduce the two key techniques that preserve the model performance of Pier. We also present the scalable design of Pier in LLM pretraining, incorporating both data parallel and tensor parallel approaches.

A. Momentum Warmup

In the original DiLoCo study, exploiting the so-called “lazy-start” technique, where training begins with AdamW then switches to DiLoCo, leads to lower model performance than the AdamW baseline [15]. The cause of the performance degradation is the training instability during the transition from AdamW to DiLoCo. To mitigate the instability issue, we design the momentum warmup technique. During the “lazy-start” phase, e.g., the first 10% of the pretraining, Pier uses AdamW in standard data parallelism. This is to leverage AdamW’s capability of quickly escaping local minima in the early stage. At the same time, Pier accumulates the momentum by differencing the models’ states with the same interval as the outer optimizer. Please note that, in the “lazy-start” phase, Pier only accumulates the momentum without applying it for model updates.

Algorithm 1 illustrates the momentum warmup technique. The default value of the momentum coefficient is $\mu = 0.9$.

Algorithm 2 Pier

Input: Train Iterations T **Input:** Warmup Percentage p **Input:** Synchronization interval r **Initialize:** Momentum coefficient μ **Initialize:** Model parameters θ **Initialize:** Momentum buffer M

```
1:  $\theta, M \leftarrow \text{MomentumWarmup}(T, p, r)$ 
2: Initialize data parallel sub-groups:  $\{\mathcal{G}_1, \mathcal{G}_2, \dots, \mathcal{G}_k\}$ 
3: for  $t = pT$  to  $T$  do
4:   if  $t \bmod r \neq 0$  then
5:     for each subgroup  $\mathcal{G}_i$  do
6:       Compute local gradient  $\nabla_\theta$ 
7:        $\theta_t \leftarrow \text{OptimizerUpdate}(\theta_{t-1}, \nabla_\theta)$ 
8:     end for
9:   else
10:     $\Delta\theta \leftarrow \theta_t - \theta_{t-r}$ 
11:     $\Delta\theta \leftarrow \text{AllReduce}(\Delta\theta)$  {across all ranks}
12:    if  $0.1T \leq t < 0.15T$  then
13:       $\mu \leftarrow 0.99$ 
14:    else if  $0.15T \leq t < 0.2T$  then
15:       $\mu \leftarrow 0.95$ 
16:    else
17:       $\mu \leftarrow 0.9$ 
18:    end if
19:     $lr \leftarrow \text{outer\_lr\_scheduler}(t)$ 
20:     $M \leftarrow \mu M + \Delta\theta$ 
21:     $\theta_t \leftarrow \theta_{t-r} + lr * (M * \mu + \Delta\theta)$ 
22:  end if
23: end for
```

With momentum warmup, Pier initializes the outer optimizer with the accumulated momentum.

B. Momentum Decay

After switching to DiLoCo, Pier incorporates the momentum decay technique for graceful transition. The intuition is to leverage the faster empirical convergence rate of AdamW compared to SGD variants with momentum, as AdamW provides a normalized and adaptive estimate of the gradient direction. Thus, Pier exploits a momentum schedule after the optimizer transition. The details are shown in Algorithm 2.

Specifically, Pier runs the “lazy start” phase for the first 10% of the overall training. Then Pier switches to DiLoCo. From 10% to 15% of total training steps, the momentum coefficient μ is set to 0.99 to avoid sharp changes in velocity during the unstable stage. From 15% to 20%, μ decays to 0.95. After 20% of the total steps, μ remains at 0.9, matching the recommended hyperparameter setting for the DiLoCo outer optimizer. In practice, we find combining the momentum warmup and decay techniques is effective in GPT model pretraining, including GPT small, medium, and XL (see §VI-A1).

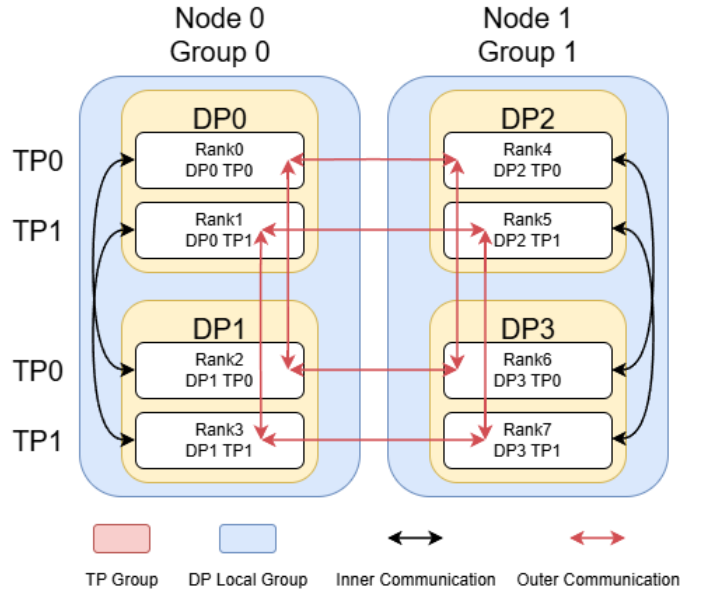


Fig. 2. Illustration of Inner- and Outer-Communication in a 2D Parallel Training Setup with Data Parallel Size of 4 and a Tensor Parallel Size of 2. There are two local communication groups, each located on a separate compute node.

C. 2D Parallelism

The design of vanilla DiLoCo [15] replaces full data parallel gradient synchronization with a low-communication alternative. However, in large-scale training, data parallelism is often combined with tensor parallelism. The complex parallelism in LLM pretraining complicates the efficient and scalable Pier design.

Following the design of Megatron-LM [6] in its tensor parallel(TP) and data parallel(DP) arrangement, Pier first ensures that TP ranks are placed within the same node whenever possible. During the lazy start phase, Pier uses AdamW in data parallel over tensor parallel, as shown in Figure 2. In this example, a model is split across two processors in every data parallel rank. Each data parallel rank (DP rank) maintains a complete copy of the model, while the model is split across two tensor parallel ranks (TP ranks). So all processors with the same TP rank have a synchronized copy of the model partition. And they can compute the momentum by comparing the changes of the current value and the previous value. The warmup momentum for the first model partition is available on all processors with TP0. And the momentum for the second model partition is available on all processors with TP1.

Upon transition, the inner optimizer (i.e., AdamW) communicates the gradients of DP0 and DP1 in Node 0. A concurrent all-reduce operation runs on DP2 and DP3 in Node 1. All the communication of inner optimizers are within a node, thus it can benefit from the high-bandwidth links, e.g., NVLink. The outer optimizer is activated periodically, e.g., for every 50 iterations. Upon activation, the outer optimizer will all-gather the model partitions among the processors with the same TP rank. In this case, the all-gather is on four processors.

This communication spans multiple nodes over low-bandwidth links, such as InfiniBand. However, global communication is only required every 50 iterations. As shown in Figure 2, the all-gather on TP ranks of 0 does not overlap with TP ranks of 1. The communication can be launched in parallel naturally, which allows for efficient utilization of the low-bandwidth links.

Although Pier only implements DP and TP, it can be easily extended to include pipeline parallelism, where the all-gather of model states can be streamlined. The current implementation is compatible with FSDP-1 (fully sharded data parallel) and FSDP-2, as FSDP-1 only distributes optimizer states over processors. Additionally, the extra model distribution strategy in FSDP-2 can be integrated in the same manner as TP.

In this paper, we demonstrate the applicability of Pier in DP and TP, highlighting the runtime speedup achieved by Pier compared to AdamW.

V. IMPLEMENTATION

We prototype Pier on top of Megatron-LM [27]. The local communication data parallel groups (referred to as groups in the following) are formed by partitioning the data parallel ranks during the communication initialization process. Pier uses AdamW as the inner optimizer within each group and Nesterov momentum as the outer optimizer across the groups. The outer synchronization (i.e., model gathering) is integrated into the main training loop by the end of each interval. To fully utilize the compute capability, Pier leverages FlashAttention-2 [28].

Our selection of outer optimizer follows the conclusion of the DiLoCo paper [15], which states that the Nesterov momentum optimizer achieves the best results. However, it is notable that there is a difference between the theoretical Nesterov momentum and the PyTorch implementation. In the original Nesterov momentum [29], the update is performed by first taking a look-ahead step in the direction of the current momentum, then computing the gradient at this anticipated position, and finally correcting the momentum and model weights based on this look-ahead gradient. However, the PyTorch implementation of Nesterov momentum [30] uses an approximated formulation, where the direction of update is efficiently adjusted by combining the momentum and the current gradient in one step, without explicitly performing the separate look-ahead gradient evaluation. We implement and test both versions, and select the PyTorch version of Nesterov momentum since it achieves better empirical performance in our setting.

The original DiLoCo work [15] suggests a fixed outer learning rate because the outer gradient is proportional to the inner update, which is already controlled by the inner learning rate scheduler. However, our empirical results show that adjusting the outer learning rate improves both the stability in the early stage and the final convergence. We introduce an outer learning rate warmup phase for the first 10% to 20% of the training, where the outer learning rate linearly increases from 0 to 1. This warmup phase stabilizes the training in the early phase.

After the warmup, the learning rate is increased to 1.1 between 20% and 80% for faster convergence; then we reduce it to 0.9 for the final 20%, since the recommended value from DiLoCo paper is 0.7, which is relatively small compared to our choices.

The outer optimizer in Pier evaluates the gradients by differencing the models’ states. Thus, it needs to store an additional version of the model, which exacerbates the already intensive memory usage. To lower the memory consumption of the outer optimizer, Pier offloads the old model to host memory. At the beginning of the outer optimizer steps, Pier reloads the old model states, gathers the latest model states, and evaluates the gradients. At the end of the outer optimizer steps, Pier will offload the latest model states to host memory and release the memory in GPUs. Under standard DP, on a compute node with multiple GPUs, each GPU partitions the model and only offloads and reloads the corresponding model shard and the outer optimizer momentum. This is to avoid redundant data movement between host memory and GPU memory. Also, Pier offloads the momentum of the outer optimizer to host memory with a similar approach to further reduce the memory footprint. We implement a switch to enable/disable CPU offload, as offload introduces a trade-off between I/O overhead and memory footprint.

VI. EXPERIMENTS

In this section, we study the convergence and scalability of Pier. Across all experiments, we pretrain GPT-2 small, medium, XL, and the 7B models on in OpenWebText dataset using mixed-precision (BF16 in models and FP32 in optimizers) from Megatron-LM. The hyperparameters of the experiments are in Table I.

TABLE I
HYPERPARAMETER SETTING. WE FOLLOWED THE HYPERPARAMETER USED IN SOPHIA [31].

HYPERPARAMETER	VALUE
INNER OPTIMIZER	ADAMW
INNER LEARNING RATE (GPT-2 SMALL, MEDIUM, XL)	4E-4, 3E-4, 1.5E-4
INNER MINIMUM LEARNING RATE	4E-5, 3E-5, 1.5E-5
ADAM BETA1	0.9
ADAM BETA2	0.999
INNER DECAY STYLE	COSINE
GLOBAL BATCH SIZE	512
TRAINING ITERATIONS	100000
INNER DECAY ITERATIONS	10000
LEARNING RATE WARMUP PROPORTION	2%
WEIGHT DECAY	0.1
CLIP GRAD	1
OUTER OPTIMIZER	NESTEROV
SYNCHRONIZATION INTERVAL H	50, 100, 200, 500
OUTER LEARNING RATE	IN SECTION V
OUTER MOMENTUM COEFFICIENT	IN SECTION IV-B
NUMBER OF GROUPS VERIFIED FOR CONVERGENCE	8, 32, 64

A. Convergence and Effectiveness Boundary

For the **convergence** study, we use the metrics of validation loss and a suite of thirteen downstream tasks. This task suite comprises eight tasks from the SuperGLUE benchmark [32], along with five additional tasks: LAMBADA,

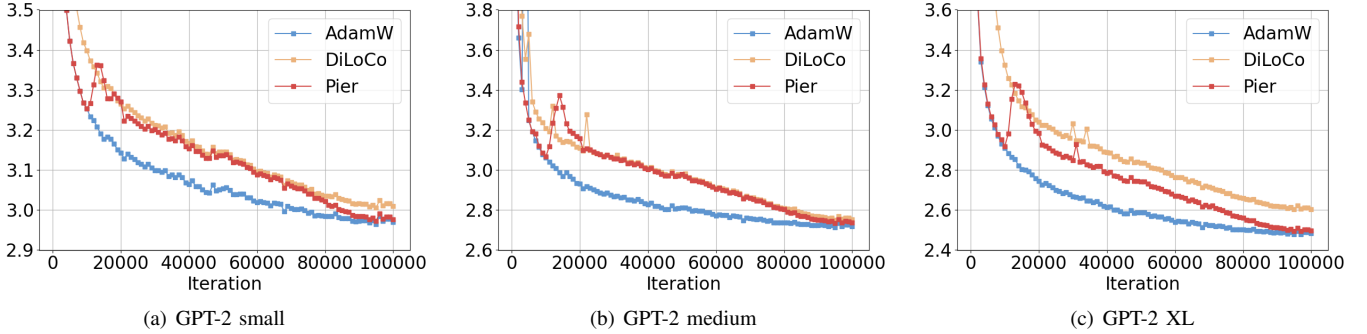


Fig. 3. Validation Loss Curves of GPT-2 Small, Medium and XL during Pretraining with AdamW, DiLoCo, and Pier. For GPT-2 small and XL, our approach achieves validation losses that are closer to those of AdamW. For GPT-2 Medium, our approach achieves lower validation loss compared to the original DiLoCo.

TABLE II

DOWNSTREAM TASKS OF GPT-2 SMALL (S), MEDIUM (M), XL MODELS PRETRAINED WITH ADAMW, DILOCO, AND PIER. MUL-RC IS MULTIRC; RCD IS RECORD; M-QA IS MATHQA; LAMB. IS LAMBADA-OPENAI; WINO. IS WINOGRAD.

METHOD	BOOLQ	CB-ACC	COPA	MUL-RC	RCD-F1	RTE	WIC	WSC	LAMB.	RACE	M-QA	PIQA	WINO.
ADAMW-S	0.5272	0.3750	0.6200	0.5474	0.7157	0.5090	0.5000	0.3558	0.3324	0.2852	0.2174	0.6148	0.4996
DiLoCo-S	0.5098	0.1964	0.6500	0.5703	0.6976	0.4838	0.5031	0.3654	0.3167	0.2804	0.2107	0.6023	0.5130
PIER-S	0.4963	0.4821	0.6400	0.5703	0.7182	0.5054	0.4953	0.3654	0.3171	0.2957	0.2141	0.6148	0.5146
ADAMW-M	0.5560	0.3750	0.6900	0.5458	0.7873	0.5307	0.4906	0.3654	0.4186	0.2986	0.2258	0.6540	0.5462
DiLoCo-M	0.5804	0.3393	0.7000	0.5336	0.7907	0.5343	0.5000	0.3750	0.4277	0.3053	0.2271	0.6431	0.5288
PIER-M	0.5872	0.5357	0.7000	0.5264	0.7953	0.5668	0.5000	0.3654	0.4120	0.2967	0.2181	0.6485	0.5478
ADAMW-XL	0.5942	0.5179	0.7400	0.4767	0.8445	0.4946	0.5016	0.4038	0.4995	0.3330	0.2332	0.6899	0.5541
DiLoCo-XL	0.6128	0.1607	0.6600	0.4878	0.8285	0.5596	0.5000	0.3654	0.4733	0.3225	0.2275	0.6746	0.5612
PIER-XL	0.5174	0.2500	0.7400	0.4775	0.8532	0.5632	0.4828	0.6346	0.5331	0.3502	0.2379	0.6986	0.5888

RACE, MathQA, PIQA, and Winograd. Throughout this study, we use two baselines: AdamW in standard data parallelism and the original DiLoCo. The convergence result is in §VI-A1. For Pier, the convergence depends on the global batch size and the synchronization interval. Thus, we perform two experiments to quantify the effectiveness boundary of the two factors. The results are reported in §VI-A2 and §VI-A3, respectively.

1) *Convergence*: The first experiment is to verify the convergence of Pier. Thus, we run full pretraining (i.e., 100,000 iterations) with AdamW, DiLoCo, and Pier. We measure the convergence using validation loss and the thirteen downstream tasks.

Figure 3 presents the validation loss curves on GPT-2 small, medium, and XL with 8, 32, 64 groups, with one GPU in each group. For Pier, we observe a clear switching point, as the model suffers from a sudden loss spike. Pier successfully mitigates the loss instability with the momentum warmup and decay techniques, showing faster convergence compared to the original DiLoCo. For GPT-2 small, the validation loss of AdamW is 2.97, compared to 3.00 of DiLoCo and 2.97 of Pier. For GPT-2 medium, the validation losses are 2.72, 2.75, and 2.74 for AdamW, DiLoCo, and Pier, respectively. For GPT-2 XL, AdamW achieves a validation loss of 2.48. The loss value of DiLoCo is 2.60 and Pier’s value is 2.49. Pier consistently achieves lower validation loss than the original DiLoCo, and the loss is comparable to the AdamW baseline.

Table II shows the downstream task performance across the three optimizers. For GPT-2 small, AdamW has five tasks with the best performance, while DiLoCo and Pier each have four and seven. For GPT-2 XL, Pier has nine tasks with the best performance, compared to three for AdamW and two for DiLoCo.

These results confirm that the convergence of Pier is comparable to AdamW. Across the three models, Pier consistently shows better downstream task performance and lower validation loss than the original DiLoCo.

2) *Global Batch Size*: In this experiment, we explore the global batch size boundary of Pier, as researchers can train the same model with more GPUs if model performance is guaranteed with larger batch sizes. We perform this experiment by pretraining GPT-2 small using weak scaling, where the global batch size increases in proportion to the GPU size. So that each GPU can maintain the same workload to sustain high utilization. To preserve fairness, we maintain a fixed budget of tokens across all scales. E.g., the number of iterations is halved with a doubled global batch size, i.e., the GPU count. So the global batch sizes on the four scales of {4, 8, 16, 32} GPUs are 256, 512, 1024, and 2048. And the numbers of iterations are 200,000, 100,000, 50,000, and 25,000.

The validation curves are shown in Figure 4. From four, eight, sixteen, to thirty-two GPUs, the validation loss increases monotonically with the values of 2.96, 2.97, 3.03, and 3.10. Ta-

ble III presents the downstream task performance across GPU counts. The model performance decreases with an increasing number of GPUs. With four GPUs (i.e., global batch size of 256), Pier has nine tasks with equal or higher performance than the AdamW baseline. This number decreases to eight on eight GPUs, seven on sixteen GPUs, and six on thirty-two GPUs.

The results confirm that the effective global batch size boundary for Pier is 512 for GPT-2 small with the model performance guarantee. We assume the same global batch size boundary for other models in the subsequent study. This is a conservative assumption, with which our subsequent study is guaranteed to converge.

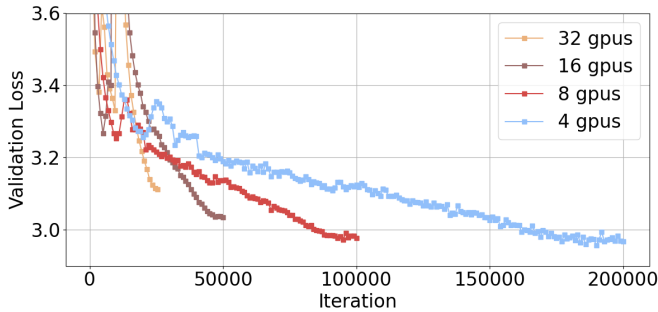


Fig. 4. Validation Loss Curves of Pier under Weak Scaling. The runs with 4 GPUs exhibit convergence. When scaling up to 16 or 32 GPUs, the validation loss rises significantly compared with the default 8 GPUs setting.

3) *Synchronization Interval*: To understand the impact of the synchronization interval in the outer optimizer on convergence, we vary the interval with $\{50, 100, 200, 500\}$ iterations on GPT-2 small pretraining. We then compare the validation loss and downstream task performance derived from each interval against the AdamW baseline (see Table II).

Table IV shows the model performance of different synchronization intervals. All four intervals show comparable validation loss values of around 2.97 at the end of the 100,000-iteration pretraining. For downstream tasks, the intervals of $\{50, 100, 200, 500\}$ have $\{8, 4, 9, 8\}$ tasks with equal or higher performance than the AdamW baseline. There is no clear pattern in the model performance across the interval range.

The results show that the convergence of Pier is less sensitive to synchronization intervals, even for extremely large intervals, such as 500 iterations.

B. Runtime Speedup

Upon confirmation of convergence, we investigate the runtime speedup patterns of Pier under various settings. In §VI-B1, we measure the runtime speedup of Pier compared to AdamW with a fixed number of groups and global batch size. In §VI-B2, we vary the number of groups while keeping the group size constant on the two GPU clusters. We report how Pier performs with data parallel and tensor parallel for LLM pretraining in §VI-B3.

To quantify runtime improvements, we evaluate three metrics. First, speedup S is the runtime ratio of the AdamW baseline ($T_{baseline}$) to our proposed method Pier (T_{Pier}):

$$S = \frac{T_{baseline}}{T_{Pier}}$$

Second, performance improvement Δp is the corresponding percentage reduction in runtime:

$$\Delta p = \frac{T_{baseline} - T_{Pier}}{T_{baseline}} \times 100\%$$

Finally, scaling efficiency e measures how well the runtime decreases for a fixed problem size as the number of processing elements increases from M to N . It's defined as:

$$e = \frac{T_M}{T_N} \times \frac{M}{N}$$

The reference value M depends on the experimental setup: in Section VI-B1, M is set to 8, 32, and 64 for the GPT-2 small, medium, and XL models, respectively; while in Section VI-B2, M is set to 1.

1) *Strong Scaling*: The previous experiments have validated the convergence property of Pier as well as the effectiveness boundary of global batch size, number of groups, and the synchronization interval in the outer optimizer. In this study, we profile the runtime speedup of Pier compared to AdamW in standard data parallelism.

The experiments run on NERSC Perlmutter, where each compute node is equipped with four NVIDIA A100 GPUs. We fix the synchronization interval at 50 iterations to estimate the lower bound of the runtime improvement. We also project the runtime reduction with an interval of 500 iterations as the upper bound estimation. The number of groups is also fixed with the empirical settings that have shown convergence. For example, Pier uses 64 groups (one GPU per group) in the convergence study in §VI-A1 for GPT-2 XL. Then we increase the group size (i.e., the number of GPUs in a group) from one, two, to four GPUs, to limit intra-group communication within a node.

Figure 5 shows the runtime measurement and scaling efficiency of GPT-2 models with Pier and AdamW. We run each experiment for 2,000 iterations, then estimate the speedup by projecting to the full 100,000-step pretraining. Please note that we set the global batch size to 512. On smaller scales, the local batch size per GPU is eight. Megatron-LM accumulates gradients to realize a larger batch size. On larger scales, such as 128 GPUs, we must lower the local batch size to four, which may result in lower utilization on each GPU, as the batch size may not saturate the GPU's computing capability. The comparison between Pier and AdamW is still fair, as the local batch size per GPU is identical in both cases. The time estimation is calculated by a weighted average, with 10% momentum warmup using AdamW in standard data parallel and 90% with Pier.

For GPT-2 models, Pier speeds up pretraining by 1.7x, 2.6x, and 2.7x for small, medium, and XL, respectively, on the largest possible scale. With the synchronization interval of 500

TABLE III

DOWNSTREAM TASKS RESULTS OF GPT-2 SMALL MODELS PRETRAINED WITH DIFFERENT NUMBER OF GPUS IN WEAK SCALING. MUL-RC IS MULTI-RC; RCD IS RECORd; M-QA IS MATHQA; LAMB. IS LAMBADA-OPENAI; WINO. IS WINOGRAD; LOSS IS VALIDATION LOSS. BOLD VALUES ARE EQUAL OR HIGHER PERFORMANCE THAN THE ADAMW BASELINE IN TABLE II.

GPU	BOOLQ	CB-ACC	COPA	MUL-RC	RCD-F1	RTE	WIC	WSC	LAMB.	RACE	M-QA	PIQA	WINO.	LOSS
4	0.5355	0.4643	0.6700	0.5631	0.7207	0.5235	0.5157	0.3462	0.3315	0.2967	0.2141	0.6094	0.5051	2.96
8	0.4963	0.4821	0.6400	0.5703	0.7182	0.5054	0.4953	0.3654	0.3171	0.2957	0.2141	0.6148	0.5146	2.97
16	0.4514	0.2679	0.6800	0.5501	0.7030	0.5307	0.5078	0.3654	0.3136	0.2823	0.2228	0.6001	0.5075	3.03
32	0.5153	0.3214	0.6500	0.5311	0.6749	0.5343	0.5000	0.3654	0.3022	0.2890	0.2097	0.6023	0.5178	3.10

TABLE IV

DOWNSTREAM TASK RESULTS OF GPT-2 SMALL MODELS PRETRAINED WITH DIFFERENT SYNCHRONIZATION INTERVALS. INT. IS SYNCHRONIZATION INTERVAL; MUL-RC IS MULTI-RC; RCD IS RECORd; M-QA IS MATHQA; LAMB. IS LAMBADA-OPENAI; WINO. IS WINOGRAD; LOSS IS VALIDATION LOSS. BOLD VALUES ARE EQUAL OR HIGHER PERFORMANCE THAN THE ADAMW BASELINE IN TABLE II.

INT.	BOOLQ	CB-ACC	COPA	MUL-RC	RCD-F1	RTE	WIC	WSC	LAMB.	RACE	MATH	PIQA	WINO.	LOSS
50	0.4963	0.4821	0.6400	0.5703	0.7182	0.5054	0.4953	0.3654	0.3171	0.2957	0.2141	0.6148	0.5146	2.97
100	0.4211	0.3571	0.6500	0.5221	0.7142	0.5018	0.4734	0.3846	0.3138	0.2919	0.2124	0.6083	0.5051	2.97
200	0.5125	0.5357	0.6200	0.5633	0.7170	0.4585	0.5000	0.3654	0.3266	0.3072	0.2157	0.6148	0.5020	2.97
500	0.4453	0.4107	0.6200	0.5660	0.7202	0.4910	0.4922	0.3942	0.3115	0.2813	0.2181	0.6192	0.5162	2.98

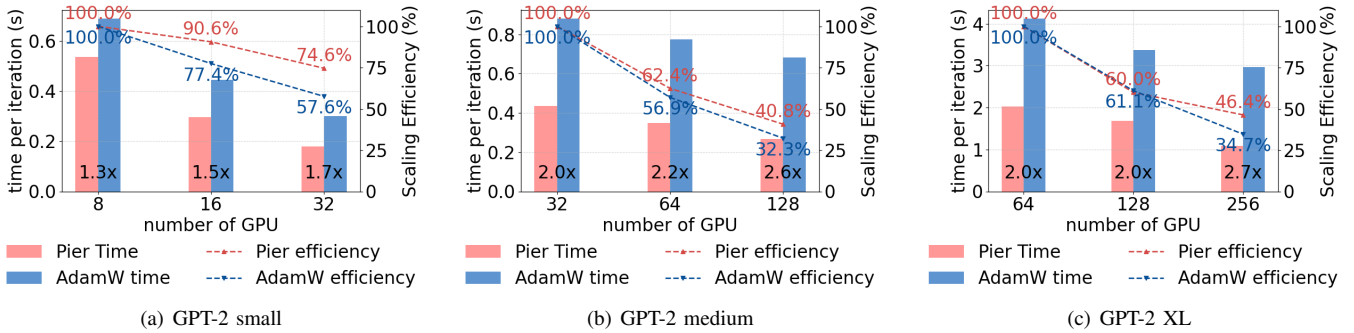


Fig. 5. Runtime and Strong Scaling Efficiency Comparison Between AdamW and Pier. The proposed method achieves up to 1.7x, 2.6x, and 2.7x speedup for pretraining of GPT-2 small, medium, and XL on the NERSC Perlmutter Cluster. Number of communication groups is set to $\{8, 32, 64\}$ in Figure 5(a), 5(b), 5(c), which has a verified convergence in VI-A1.

iterations, the speedup of Pier on GPT-2 XL is 2.2x, 2.2x, and 3.7x on 64, 128, and 256 A100s, as shown in Figure 6. The sustained scaling efficiency is 57.9% compared to 34.7% for AdamW on 256 A100s.

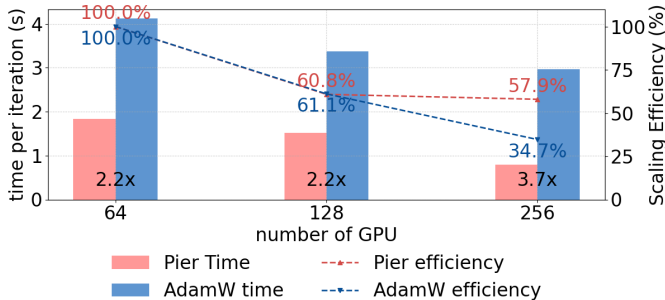
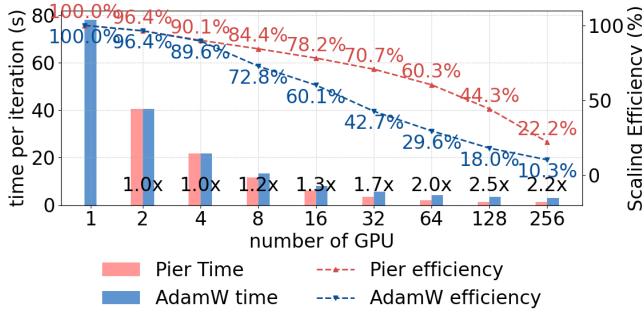


Fig. 6. Runtime and Strong Scaling Efficiency Comparison between AdamW and Pier. The experiment follows the same basic setting as in Figure 5(c), but Pier achieves better results with a synchronization interval of 500.

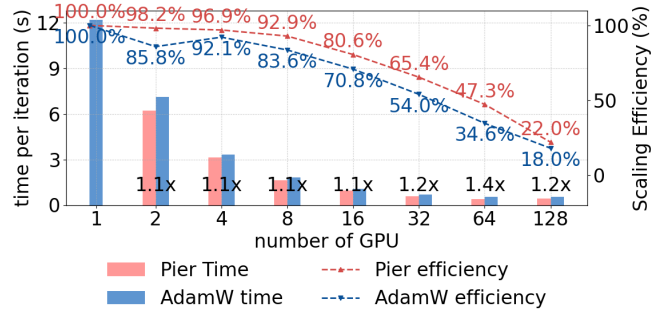
2) *Performance: Varying number of groups:* In this experiment, we examine the runtime performance gain when each GPU is considered as a group. This setting completely eliminates the communication in the inner optimizer. We fix the global batch size across scales for convergence guarantee. We measure the speedup on both NERSC Perlmutter and TACC Vista.

Figure 7 shows the measurements of GPT-2 XL. On Perlmutter, Pier achieves significant speedups beyond one compute node (i.e., four GPUs). The speedup increases monotonically from 4 to 128 GPUs, then decreases at 2.2x on 256 A100s. The scaling efficiency is 70.7%, which is drastically higher than the 42.7% achieved by AdamW at the same scale. On Vista, Pier is more effective at larger scales. E.g., Pier shows a speedup of 1.4x and 1.2x on 64 GH200s and 128 GH200s, respectively.

With a further relaxed communication interval of 500 iterations, the speedup in runtime is 1.8x and 1.9x for Pier on 64 and 128 GH200s, respectively. The relatively lower speedup



(a) Perlmutter



(b) Vista

Fig. 7. Runtime and Scaling Efficiency Comparison between AdamW and Pier of GPT-2 XL Pretraining, where the number of communication groups equals to the number of GPUs. The proposed method achieves up to 2.5x speedup using 128 A100 GPUs on Perlmutter, and up to 1.4x speedup when using 64 GH200 GPUs on Vista. The scaling efficiency is calculated based on the runtime of AdamW with 1 GPU.

on Vista compared to Perlmutter can be attributed to the machine configuration. On Vista, each node is equipped with one GH200 superchip, and the network is Infiniband NDR, which offers a bandwidth of 400 Gbps. The network is shared with 256 CPU nodes and 600 GPU nodes. In contrast, the compute node on Perlmutter has four A100 GPUs connected by NVLink, and the network is Slingshot 11 with four NICs per node. The network is shared by 3,072 CPU nodes and 1,792 GPU nodes. The scaling efficiency of GPT-2 XL on 64 GH200 GPUs is reported as 34.6% for AdamW. Pier’s scaling efficiency is 47.3% on the same scale, which is 36.7% higher than AdamW

With the synchronization interval of 50 iterations, the scaling efficiency of Pier drops below 40% beyond 64 GH200s and 128 A100s, which are the efficient scaling boundaries for GPT-2 XL. The boundary depends on the model, the synchronization interval, the computing capability of GPUs, and the networks.

3) *Performance: Scale with Tensor Parallel:* All previous experiments in this section examine the runtime improvement of Pier in data parallel. In this experiment, we measure the runtime speedup of Pier in the setting of combined data parallel (DP) and tensor parallel (TP). We perform this experiment on Perlmutter and set TP to four, as each compute node has four A100s. We use a GPT-2 model with 7B parameters, which is the maximum that can be hosted across four 40 GB A100s. The scaling baseline is measured with one node. Our test case runs on 32 nodes (i.e., 128 A100s).

From the measurements, we observe that Pier runs 2.2x faster than AdamW on 128 A100s. The sustained scaling efficiency of Pier is 73.4% compared at 33.4% of AdamW. The results show that, in addition to data parallelism, Pier is effective in reducing runtime cost with complex parallelism for LLM pretraining.

VII. CONCLUSION

We present Pier, an optimization framework for LLM pretraining with relaxed global communication. Pier is enabled by the momentum warmup and momentum decay algorithms, and

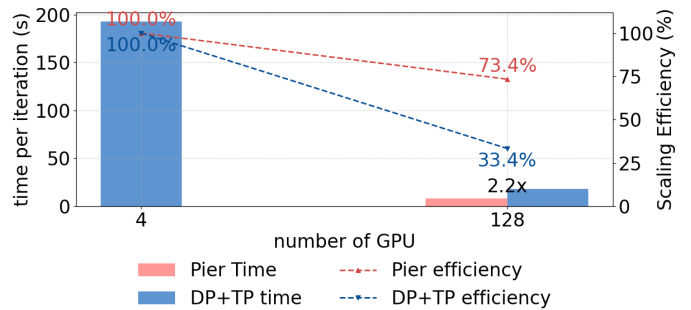


Fig. 8. Runtime and Scaling Efficiency Comparison between DP+TP and Pier. With a TP rank of 4, our approach achieves 2.2x speedup when scaling to 32x more GPUs.

an efficient and scalable system design to address complex parallel strategies in LLM pretraining. We verify the convergence properties of Pier and identify the effectiveness boundary of global batch size, number of groups, and synchronization intervals. We measure the speedup of Pier compared to the widely adopted AdamW optimizer across machines, scales, and models. The results show that Pier can speed up LLM-pretraining by 2.2x-3.7x for GPT-2 XL on 256 A100s on Perlmutter. Pier also exhibits a 2.2x speedup for GPT-2 7B on 256 A100s. On Vista, Pier reduces the end-to-end time cost of GPT-2 XL by 18.3-46.8% on 128 GH200s. Pier is a strong optimization framework candidate in LLM pretraining, as it achieves significant speedups while preserving model performance.

REFERENCES

- [1] J. Kaplan, S. McCandlish, T. Henighan, T. B. Brown, B. Chess, R. Child, S. Gray, A. Radford, J. Wu, and D. Amodei, “Scaling laws for neural language models,” *arXiv preprint arXiv:2001.08361*, 2020.
- [2] T. Brown, B. Mann, N. Ryder, M. Subbiah, J. D. Kaplan, P. Dhariwal, A. Neelakantan, P. Shyam, G. Sastry, A. Askell, S. Agarwal, A. Herbert-Voss, G. Krueger, T. Henighan, R. Child, A. Ramesh, D. Ziegler, J. Wu, C. Winter, C. Hesse, M. Chen, E. Sigler, M. Litwin, S. Gray, B. Chess, J. Clark, C. Berner, S. McCandlish, A. Radford, I. Sutskever, and D. Amodei, “Language Models are Few-Shot Learners,” in *Advances in Neural Information Processing Systems*, ser. NeurIPS, H. Larochelle, M. Ranzato, R. Hadsell, M. F. Balcan, and

- H. Lin, Eds., vol. 33. Red Hook, NY, USA: Curran Associates, Inc., 2020, pp. 1877–1901. [Online]. Available: <https://proceedings.neurips.cc/paper/2020/file/1457c0d6bfc4967418bf8ac142f64a-Paper.pdf>
- [3] Z. Jiang, H. Lin, Y. Zhong, Q. Huang, Y. Chen, Z. Zhang, Y. Peng, X. Li, C. Xie, S. Nong *et al.*, “{MegaScale}: Scaling large language model training to more than 10,000 {GPUs},” in *21st USENIX Symposium on Networked Systems Design and Implementation (NSDI 24)*, 2024, pp. 745–760.
 - [4] A. Grattafiori, A. Dubey, A. Jauhri, A. Pandey, A. Kadian, A. Al-Dahle, A. Letman, A. Mathur, A. Schelten, A. Vaughan *et al.*, “The llama 3 herd of models,” *arXiv preprint arXiv:2407.21783*, 2024.
 - [5] S. Li, Y. Zhao, R. Varma, O. Salpekar, P. Noordhuis, T. Li, A. Paszke, J. Smith, B. Vaughan, P. Damania *et al.*, “Pytorch distributed: Experiences on accelerating data parallel training,” *arXiv preprint arXiv:2006.15704*, 2020.
 - [6] M. Shoeybi, M. Patwary, R. Puri, P. LeGresley, J. Casper, and B. Catanzaro, “Megatron-lm: Training multi-billion parameter language models using model parallelism,” *arXiv preprint arXiv:1909.08053*, 2019.
 - [7] Y. Huang, Y. Cheng, A. Bapna, O. Firat, D. Chen, M. Chen, H. Lee, J. Ngiam, Q. V. Le, Y. Wu *et al.*, “Gpipe: Efficient training of giant neural networks using pipeline parallelism,” *Advances in neural information processing systems*, vol. 32, 2019.
 - [8] D. Narayanan, A. Harlap, A. Phanishayee, V. Seshadri, N. R. Devanur, G. R. Ganger, P. B. Gibbons, and M. Zaharia, “Pipedream: Generalized pipeline parallelism for dnn training,” in *Proceedings of the 27th ACM symposium on operating systems principles*, 2019, pp. 1–15.
 - [9] H. Liu, M. Zaharia, and P. Abbeel, “Ring attention with blockwise transformers for near-infinite context,” *arXiv preprint arXiv:2310.01889*, 2023.
 - [10] Y. Lin, S. Han, H. Mao, Y. Wang, and W. J. Dally, “Deep gradient compression: Reducing the communication bandwidth for distributed training,” in *International Conference on Learning Representations (ICLR)*, 2018.
 - [11] M. Zheng and Z. Zhang, “Radius: Range-based gradient sparsity for large foundation model pre-training,” in *Eighth Conference on Machine Learning and Systems*, 2025.
 - [12] F. Faghri, I. Tabrizian, I. Markov, D. Alistarh, D. M. Roy, and A. Ramezani-Kebrya, “Adaptive gradient quantization for data-parallel sgd,” *Advances in neural information processing systems*, vol. 33, pp. 3174–3185, 2020.
 - [13] S. U. Stich, “Local sgd converges fast and communicates little,” *arXiv preprint arXiv:1805.09767*, 2018.
 - [14] J. Song, J. Yim, J. Jung, H. Jang, H.-J. Kim, Y. Kim, and J. Lee, “Optimus-CC: Efficient Large NLP Model Training with 3D Parallelism Aware Communication Compression,” in *Proceedings of the 28th ACM International Conference on Architectural Support for Programming Languages and Operating Systems, Volume 2*, ser. ASPLOS 2023. New York, NY, USA: Association for Computing Machinery, 2023, p. 560–573. [Online]. Available: <https://doi.org/10.1145/3575693.3575712>
 - [15] A. Douillard, Q. Feng, A. A. Rusu, R. Chhaparia, Y. Donchev, A. Kuncoro, M. Ranzato, A. Szlam, and J. Shen, “Diloco: Distributed low-communication training of language models,” *arXiv preprint arXiv:2311.08105*, 2023.
 - [16] A. Gokaslan and V. Cohen, “Openwebtext corpus,” <https://github.com/jcpeterson/openwebtext>, 2019, an open-source recreation of the OpenAI WebText dataset.
 - [17] S. Li, F. Xue, C. Baranwal, Y. Li, and Y. You, “Sequence parallelism: Long sequence training from system perspective,” 2022.
 - [18] H. Liu and P. Abbeel, “Blockwise parallel transformers for large context models,” *Advances in Neural Information Processing Systems*, vol. 36, 2024.
 - [19] F. Seide, H. Fu, J. Droppo, G. Li, and D. Yu, “1-bit stochastic gradient descent and its application to data-parallel distributed training of speech dnns,” in *Interspeech*, 2014.
 - [20] P. Richtárik, N. Sokolovska, A. Sahu, N. Loizou, A. Gruntkowska, S. Horyáth, and K. Mishchenko, “Ef21: A new, simpler, theoretically better, and practically faster error feedback,” in *Advances in Neural Information Processing Systems (NeurIPS)*, 2021.
 - [21] Y. Tsuzuku, H. Imachi, and T. Akiba, “Variance-based gradient compression for efficient distributed deep learning,” *arXiv preprint arXiv:1802.06058*, 2018.
 - [22] T. Vogels, S. P. Karimireddy, and M. Jaggi, “Powersgd: Practical low-rank gradient compression for distributed optimization,” in *Advances in Neural Information Processing Systems (NeurIPS)*, 2019.
 - [23] E. Gorbunov, F. Hanzely, and P. Richtárik, “Local sgd: Unified theory and new efficient methods,” in *International Conference on Artificial Intelligence and Statistics*. PMLR, 2021, pp. 3556–3564.
 - [24] Z. Charles, G. Teston, L. Dery, K. Rush, N. Fallen, Z. Garrett, A. Szlam, and A. Douillard, “Communication-efficient language model training scales reliably and robustly: Scaling laws for diloco,” *arXiv preprint arXiv:2503.09799*, 2025.
 - [25] A. Sarfi, B. Thérien, J. Lidin, and E. Belilovsky, “Communication efficient llm pre-training with sparseloco,” *arXiv preprint arXiv:2508.15706*, 2025.
 - [26] A. Douillard, Y. Donchev, K. Rush, S. Kale, Z. Charles, Z. Garrett, G. Teston, D. Lacey, R. McIlroy, J. Shen *et al.*, “Streaming diloco with overlapping communication: Towards a distributed free lunch,” *arXiv preprint arXiv:2501.18512*, 2025.
 - [27] NVIDIA Corp., “Megatron-LM & Megatron Core,” <https://github.com/NVIDIA/Megatron-LM>, 2025.
 - [28] T. Dao, “Flashattention-2: Faster attention with better parallelism and work partitioning,” *arXiv preprint arXiv:2307.08691*, 2023.
 - [29] Y. Nesterov, “A method for solving the convex programming problem with convergence rate $o(1/k^2)$,” in *Dokl akad nauk Sssr*, vol. 269, 1983, p. 543.
 - [30] PyTorch Contributors, “torch.optim.SGD — pytorch documentation,” <https://docs.pytorch.org/docs/stable/generated/torch.optim.SGD.html>, 2025.
 - [31] H. Liu, Z. Li, D. Hall, P. Liang, and T. Ma, “Sophia: A scalable stochastic second-order optimizer for language model pre-training,” *arXiv preprint arXiv:2305.14342*, 2023.
 - [32] A. Wang, Y. Pruksachatkun, N. Nangia, A. Singh, J. Michael, F. Hill, O. Levy, and S. Bowman, “Superglue: A stickier benchmark for general-purpose language understanding systems,” *Advances in neural information processing systems*, vol. 32, 2019.